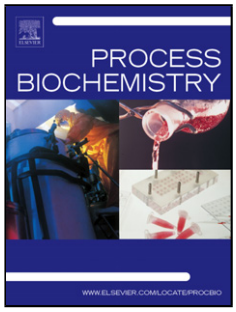


Title: Enzymatic production of key intermediate of gabapentin by recombinant amidase from *Pantoea* sp. with high ratio of substrate to biocatalyst

Author: Zhe-Ming Wu Ren-Chao Zheng Xu Ding Jian-Qiang Jin Yu-Guo Zheng

PII: S1359-5113(16)30025-3
DOI: http://dx.doi.org/doi:10.1016/j.procbio.2016.02.012
Reference: PRBI 10626

To appear in: *Process Biochemistry*

Received date: 26-12-2015
Revised date: 6-2-2016
Accepted date: 23-2-2016

Please cite this article as: Wu Zhe-Ming, Zheng Ren-Chao, Ding Xu, Jin Jian-Qiang, Zheng Yu-Guo.Enzymatic production of key intermediate of gabapentin by recombinant amidase from Pantoea sp.with high ratio of substrate to biocatalyst.*Process Biochemistry* http://dx.doi.org/10.1016/j.procbio.2016.02.012

# Enzymatic production of key intermediate of gabapentin by recombinant amidase from *Pantoea* sp. with high ratio of substrate to biocatalyst

**Authors and Affiliation:**

Zhe-Ming Wu[a,b], Ren-Chao Zheng[a,b], Xu Ding[a,b], Jian-Qiang Jin[a,b] and Yu-Guo Zheng[a,b]*

[a]*Key Laboratory of Bioorganic Synthesis of Zhejiang Province, College of Biotechnology and Bioengineering, Zhejiang University of Technology, Hangzhou 310014, P. R. China*

[b]*Engineering Research Center of Bioconversion and Biopurification of Ministry of Education, Zhejiang University of Technology, Hangzhou 310014, P. R. China*

***Corresponding author:**

Tel: +86-571-88320630, Fax: +86-571-88320630, E-mail: zhengyg@zjut.edu.cn

## Graphical abstract

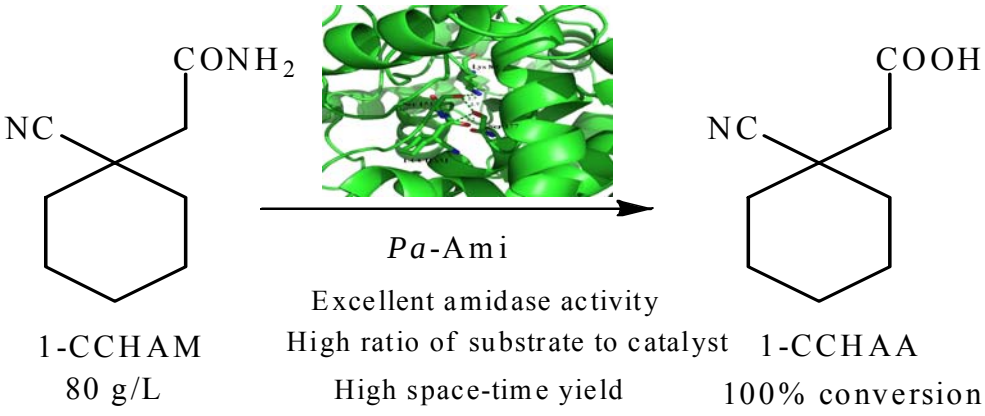

Highlights:

1. A novel bioprocess for preparing 1-cyanocyclohexaneacetic acid was developed.
2. Three amidases were investigated to hydrolyze 1-cyanocyclohexaneacetamide.
3. *Pa*-Ami exhibited high activity (297.6 U/mg) and catalytic efficiency.
4. *Pa*-Ami-catalyzed process afforded a space-time yield of 5794.7 $g_{product}$ $L^{-1}$ $d^{-1}$.
5. *Pa*-Ami was inhibited by 1-cyanocyclohexaneacetic acid.

Abstract: 1-Cyanocyclohexaneacetic acid is the key intermediate of gabapentin. A novel bioprocess catalyzed by amidase was developed for efficient production of 1-cyanocyclohexaneacetic acid from 1-cyanocyclohexaneacetamide, which can be prepared with high efficiency by nitrile hydratase-catalyzed regioselective hydration of 1-cyanocyclohexaneacetonitrile. Kinetic analysis and molecular docking of three recombinant amidase demonstrated that amidase (*Pa*-Ami) from *Pantoea* sp. was the most robust biocatalyst for hydrolysis of 1-cyanocyclohexaneacetamide with the $k_{cat}/K_m$ value of 208.2±16.2 $mM^{-1}$ $s^{-1}$. Some key parameters of the bioprocess, such as substrate loading, catalyst loading and product inhibition, were investigated. Enzymatic hydrolysis of 80 g/L of 1-cyanocyclohexaneacetamide was completed within 20 min using 1 g/L wet whole cells of recombinant *Escherichia coli* BL21, leading to high ratio of substrate to catalyst (S/C-ratio, 80) and high space-time yield (5794.7 $g_{product}$ $L^{-1}$ $d^{-1}$). These encouraging results indicated the great potential of *Pa*-Ami in practical production of gabapentin.

Keywords: Amidase, Gabapentin, Whole-cell biocatalysis, High space-time yield, Hydrolysis

## 1. Introduction

Gabapentin, initially known as antiepileptic drug (AED) in 1994, is a structural analog of inhibitory neurotransmitter γ-aminobutyric acid (GABA) [1]. It has been approved for the treatment of neuropathic pain related to postherpetic neuralgia [2], postpoliomyelitis neuropathy [3], and reflex sympathetic dystrophy [4]. Due to its acceptable side effects and strong safety record, gabapentin is currently touted as one of the most popular drugs [5, 6].

With the increasing demand of gabapentin in recent years, several chemical routes have been developed from readily available raw materials [7, 8]. 1-Cyanocyclohexaneacetic acid (1-CCHAA) is a key intermediate of gabapentin. One developed chemical process via formation of 1-CCHAA as intermediate from 1-cyanocyclohexylacetonitrile (1-CCHAN) and followed by hydrogenation, was approved as an attractive approach for gabapentin [9, 10]. However, the chemical process typically required drastic conditions and produced unwanted by-products and considerable amount of inorganic wastes. Furthermore, ω-cyanocarboxylic acid 1-CCHAA was produced in low purity and yield due to poor regioselectivity of chemical hydrolysis of α,ω-dinitrile 1-CCHAN. An alternative approach to the ω-cyanocarboxylic acid is the selective hydrolysis of dinitrile catalyzed by nitrilases [11-14]. However, some practical problems such as low substrate concentration and high biocatalyst loading restricted its industrial applications. Recently, a bioprocess for regioselective hydration of 1-CCHAN was developed using *Rhodococcus aetherivorans* ZJB1208 nitrile hydratase in our laboratory, and the concentration of

product (1-cyanocyclohexaneacetamide, 1-CCHAM) accumulated as high as 966.7 g. $L^{-1}$ [15]. Since the selective chemical hydrolysis of cyano and amide bond of 1-CCHAM is virtually impossible, amidase-catalyzed hydrolysis is the only facile way of preparing 1-CCHAA from 1-CCHAM (Fig. 1). Moreover, nitrile hydratase-amidase coupled biotransformation will provide a particularly appealing approach [16].

In our effort to search for efficient biocatalysts, three signature amidase (AS) family amidases (*Pa*-Ami from *Pantoea* sp., *Cc*-Ami from *Comamonas composti* and *Dt*-Ami 6 from *Delftia tsuruhatensis* ZJB-05174) have been exploited for their hydrolytic activity towards 1-CCHAM. *Pa*-Ami was found to exhibit highest catalytic efficiency, indicating its great potential in large-scale production of 1-CCHAA for gabapentin synthesis.

## 2. Materials and methods

### *2.1 Chemicals*

Compounds 1-CCHAN and 1-CCHAA were provided by Zhejiang Chiral Medicine Chemicals Co., Ltd. (Hangzhou, China). Compound 1-CCHAM was prepared using 1-CCHAN as substrate by *R. aetherivorans* preserved in our laboratory [15]. Isopropyl-β-D-thiogalactopyranoside (IPTG) and kanamycin were purchased from Sigma. All other chemicals were of analytical grade and purchased from commercial sources.

### *2.2 Construction of recombinant vectors*

The genomic DNA of *D. tsuruhatensis* ZJB-05174 was extracted and used as

template, and two sets of primers (1 μM each) *Dt*-Ami 6-F (5'-CATATGAACGACAGCGAACTGCACC-3') and *Dt*-Ami 6-R (5'-AAGCTTTCAGGCAGCAGGGTGCTGTCTGT-3') were used to amplify the *Dt*-Ami 6 gene (GenBank accession no. KP943494). The reaction system (100 μL) contained 4 U *Taq* DNA polymerase, 40 ng genomic DNA, 100 μM each dNTP, and 10 μL 10 × *Taq* DNA buffer. The PCR program was carried out as follows: 94 °C for 3 min; followed by 30 cycles at 94 °C for 30 s, 58 °C for 30 s, and 72 °C for 2 min; the reaction was further carried out at 72 °C for 10 min and finally kept at 4 °C. The DNA fragment was digested with *Nde*I and *Hin*dⅢ and ligated to the pre-digested pET-28a(+) with the same restriction enzymes. After confirming the absence of unintended mutations, the plasmid was introduced into *E. coli* BL21(DE3).

The amino acid sequences of *Pa*-Ami (GenBank accession no. WP_008109374) and *Cc*-Ami (GenBank accession no. WP_027015397) were reverse-translated on the basis of the preferred codons by gene designer software against *E. coli* as host[17]. The synthesized genes with 6 × His-tag were inserted into expression vector pET-28a(+) between *Nco*I and *Eco*RI restriction endonuclease sites. The ligated plasmids pET28a(+)-amidases were transformed into *E. coli* BL21 (DE3) by heat shock method [18].

*2.3 Expression and purification of recombinant amidases*

*E. coli* cells harboring the recombinant plasmids were grown at 37 °C in Luria-Bertani (LB) medium (peptone 10 g/L, yeast extract 5 g/L, NaCl 10 g/L) containing kanamycin (50 μg/mL) until the optical density at 600 nm reached ~0.6.

The expression of recombinant amidases were induced by 0.1 mM IPTG for 12 h at 28 °C. The cells were collected by centrifugation at 12,000 × *g* for 10 min and washed twice with Tris-HCl buffer (20 mM, pH 8.0). The harvested cells (3.0 g, wet weight) were then suspended in 30 mL Tris-HCl buffer (20 mM, pH 8.0) and disrupted by sonication with a Vibra-Cell VC 505 ultrasonic processor (Sonics and Materials Inc., Newtown, CT) at 300W for 15 min. Cell debris were removed by centrifugation at 12,000 × *g* for 20 min at 4 °C. The supernatant was used as crude extract and loaded onto a nickel-nitrilotriacetic acid (Ni-NTA) superflow column pre-equilibrated with 20 mM Tris-HCl buffer (pH 8.0). After eluting the unbound proteins with 20 mM Tris-HCl buffer (pH 8.0) containing 0.5 M NaCl and 20 mM imidazole, the bound recombinant amidases were eluted with 20 mM Tris-HCl buffer (pH 8.0) containing 0.3 M NaCl and 0.3 M imidazole. The collected fractions were dialyzed in 20 mM Tris-HCl buffer (pH 8.0) overnight at 4 °C and analyzed by 12% sodium dodecyl sulfate-polyacrylamide gel electrophoresis (SDS-PAGE).

*2.4 Enzyme assays*

The amidase activity was assayed at 45 °C by monitoring the formation of 1-CCHAA. The standard reaction mixture consisted of 20 mM Tris-HCl buffer (pH 8.0), 20 mM 1-CCHAM and an appropriate amount of the enzyme in a total volume of 1 mL. The reactions were stopped by addition of 50 μL HCl (1 M). The mixtures were centrifuged at 14,000 × *g* for 5 min and the concentration of 1-CCHAA was then analyzed by high-performance liquid chromatography (HPLC) using a ODS column (Elite, 250 × 4.6 mm) and a UV detector at 215 nm. The mobile phase consisted of

76% buffer (containing 0.58 g/L $NH_4H_2PO_4$ and 1.83 g/L $NaClO_4$, pH=1.8) and 24% acetonitrile and the flow rate was 1 mL/min. One unit of enzyme activity was defined as the amount of enzyme that catalyzed the formation of 1 μmol of 1-CCHAA per min. Protein concentrations were determined by the method of Bradford [19] using BSA as the protein standard.

*2.5 Effects of temperature and pH on Pa-Ami activity*

The reactions were performed in standard reaction mixtures (1 mL) containing 20 mM 1-CCHAM and an appropriate amount of purified *Pa*-Ami. The effect of temperature on *Pa*-Ami activity was investigated in 20 mM Tris-HCl buffer (pH 8.0) at different temperatures (30-65 °C). The optimum pH was determined at various pHs: $Na_2HPO_4$-$NaH_2PO_4$ (pH 6.0 to 7.5), Tris-HCl (pH 7.5 to 9.0) and Gly-NaOH (pH 9.0 to 10.0) under the standard assay conditions. All experiments were carried out in triplicate.

2.6 *Kinetic analysis*

Kinetic parameters were determined by measuring the enzyme activity at different substrate concentrations (0.5-20 mM). The reaction was stopped after 15 min to ensure that less than 10% of the substrate was consumed. All measurements were performed in 20 mM Tris-HCl buffer (pH 8.0) with an appropriate amount of amidase at 45 °C. The $K_m$ and $V_{max}$ were calculated from the Lineweaver-Burk double-reciprocal plot of the obtained data.

Inhibition kinetic parameters (*Ki*) were determined at 20 and 40 mM 1-CCHAM in the presence of different concentrations of 1-CCHAA (7.5 to 250 mM). Dixon plots

were adapted to determine the inhibition type.

*2.7 Homology Modeling and Molecular Docking*

The three-dimensional (3D) structures of amidases were constructed using the Build Homology Models (MODELER) module in Discovery Studio (DS) version 2.1 (Accelrys, Inc.). The crystal structure of amidase from *Thermus thermophilus* (PDB 2DC0) was used as the template for *Pa*-Ami, *Cc*-Ami and *Dt*-Ami 6 according to the results of blast. The loop of the generated 3D models were refined sufficiently using Modeller 9v4. The molecular dockings were performed using Autodock version 4.0.1 and the protein structure diagrams were prepared with PyMOL [20].

*2.8 Hydrolysis of* 1-CCHAM *catalyzed by whole cells of recombinant E. coli overexpressing Pa-Ami*

Hydrolysis of 1-CCHAM catalyzed by the recombinant *E. coli* cells overexpressing *Pa*-Ami was performed in 50 mL flasks containing 10 mL of reaction mixtures at 35 °C with stirring (180 rpm). The effect of substrate concentration on enzymatic hydrolysis was determined with the reaction mixture containing 100 mM Tris-HCl buffer (pH 8.5), 2 g/L (wet cell weight) resting cells and various concentrations of 1-CCHAM (60-100 g/L). The optimal catalyst loading was evaluated with 1-3 g/L resting cells at a substrate concentration of 100 g/L. The effect of product on hydrolysis was investigated in a reaction mixture consisted of 100 mM Tris-HCl buffer (pH 8.5), 1 g/L (wet cell weight) resting cells, 80 g/L 1-CCHAM and 10-40 g/L 1-CCHAA. Samples (900 μL) were drawn at regular intervals and the reaction was quenched by the addition of 100 μL 1M HCl. After appropriate dilution

and centrifugation (14,000 × *g*, 10 min), 100 μL of supernatant was then withdrawn and analyzed by HPLC as described above.

## 3. Results and discussion

### *3.1 Expression and purification of amidases*

Amidases can be assigned into amidase signature (AS) family and nitrilase superfamily based on their amino acid sequence [21]. The amidase signature family is defined by the AS sequence, which consist of a highly conserved stretch of approximately 130 serine- and glycine-rich amino acids and a catalytic triad of Ser-Ser-Lys (Fig. S1). Members from AS family usually display hydrolytic activity towards a broad spectrum of amides [22, 23].

*D. tsuruhatensis* ZJB-05174 was an amidase producing strain previously isolated in our laboratory [24]. Based on the AS sequence and the available genome sequence data of *D. acidovorans* SPH-1, which shared high homology with *D. tsuruhatensis*, an AS family enzyme *Dt*-Ami 6 was mined from *D. tsuruhatensis* ZJB-05174 and overexpressed in *E. coli*. As *Dt*-Ami 6 exhibited high hydrolytic activity towards 1-CCHAM **(**175.1 U/mg**)**, several homologous AS amidases which possessing a catalytic triad of Ser-Ser-Lys in AS sequence were selected, synthesized and overexpressed in *E. coli* (Fig. S1). *Pa*-Ami and *Cc*-Ami, which shared 63% and 89% identity with *Dt*-Ami 6, showed hydrolytic activity towards 1-CCHAM. Under the standard assay conditions, the specific activity of *Pa*-Ami (297.6 U/mg) was superior to those of *Dt*-Ami 6 and *Cc*-Ami (41.5 U/mg).

The recombinant enzymes were purified to homogeneity by Ni-NTA affinity

chromatography. SDS-PAGE analysis of the purified *Dt*-Ami 6, *Pa*-Ami and *Cc*-Ami showed single band corresponding to a molecular mass of about 50, 55 and 50 kDa, respectively, which were consistent with the molecular weight (49.9 kDa of *Dt*-Ami 6, 57.2 kDa of *Pa*-Ami and 51.1 kDa of *Cc*-Ami) calculated from the amino acid sequence (Fig. S2).

*3.2 Kinetic analysis*

Kinetic studies of *Pa*-Ami, *Cc*-Ami and *Dt*-Ami 6 were performed by measuring initial velocities in the presence of varying concentrations of 1-CCHAM. As shown in Table 1. *Pa*-Ami showed the lowest apparent $K_m$ value (1.21±0.11 mM) and highest $k_{cat}$ (250.1±3.5 $s^{-1}$). The catalytic efficiency of *Pa*-Ami ($k_{cat}/K_m$=208.2±16.2 $mM^{-1}$ $s^{-1}$) was about 2.3-fold higher than that of *Dt*-Ami 6. These catalytic properties suggested *Pa*-Ami as a robust biocatalyst for hydrolysis of 1-CCHAM.

*3.3 Homology Modeling and Molecular Docking*

Several models were obtained and evaluated by Procheck (http://nihserver.mbi.ucla.edu/SAVES/). The best quality models were shown in the Ramachandran plot, where 90.3%, 91.1% and 90.2% of residues were located in the most favored regions, 7.4%, 7.7% and 7.0% of residues in the additional allowed regions, 3.1%, 0.8% and 1.5% of residues in the generously allowed regions, and 0.7%, 0.5% and 0.0% in the disallowed regions for *Pa*-Ami, *Cc*-Ami and *Dt*-Ami 6, respectively. And the root-mean-square deviations between the models and 2DC0 crystal structure were 0.247, 0.210 and 0.222 for *Pa*-Ami, *Cc*-Ami and *Dt*-Ami 6, respectively. These data indicated that the constructed models were reliable.

The amidase signature family enzymes possess a catalytic Ser-Ser-Lys triad [25], and these residues are conserved in *Pa*-Ami (Ser153, Ser177 and Lys80), *Cc*-Ami (Ser155, Ser179 and Lys82) and *Dt*-Ami 6 (Ser155, Ser179 and Lys82) (Fig. 2). Based on the proposed reaction mechanism of AS amidase [26], *Pa*-Ami for example, the side-chain oxygen atom of Ser177 played a role of a nucleophilic agent and attacked the carbonyl carbon atom of the substrate. Simultaneously, carbonyl group in substrate was protonated by Ser153, which in turn deprotonated Ser177. The protonated Lys80 decreased the nucleophilic character of Ser153 and increased the ability of Ser153 to protonate the carbonyl oxygen of the substrate and the ability of Ser177 to protonate the leaving group of the substrate. Next, the amino group captured the proton from Ser153 and the Ser was protonated by the ammonium ($NH_3^+$) group at Lys. The amino group of the amide function was eliminated, the proton of the hydroxyl group in the tetrahedral enzyme–substrate intermediate was abstracted by Ser153, and the carbonyl group in the substrate molecule was restored. Finally, the Ser177 abstracted a proton from water molecular to return the original form and deprotonated water molecular attack the electrophilic carbonyl C to release the corresponding acid.

When the substrate 1-CCHAM was docked into the active site of *Pa*-Ami, *Cc*-Ami and *Dt*-Ami 6, as shown in Fig. 2, the distance between the $O^{\gamma}$ of Ser179 in *Cc*-Ami, Ser177 in *Pa*-Ami and Ser179 in *Dt*-Ami 6 and the amide carbon of the substrate were 3.5 Å, 3.2 Å, and 3.3 Å (Table S1), respectively. Because of the shorter distance, the nucleophile attack from $O^{\gamma}$ of Ser was facilitated and the catalytic

efficiency was improved. Furthermore, the efficiency of the proton relay network of catalytic triad was also an important issue and was closely related to the activity. The molecular docking data indicated that *Pa*-Ami have better proton transformation ability than *Dt*-Ami 6 and *Cc*-Ami. Therefore, *Pa*-Ami was regarded to exhibit the highest activity due to the shortest nucleophilic attack distance and best proton transfer ability, which was in accord with the determined enzyme activities.

*3.4 Effects of pH and temperature on Pa-Ami activity*

As shown in Fig. 3, *Pa*-Ami showed high activity (>90%) towards 1-CCHAM at pH ranging from 7.0 to 9.0 and the optimum pH was found to be 8.5 in Tris-HCl buffer. However, a remarkable decrease in hydrolytic activity of *Pa*-Ami was observed under acidic and basic conditions. *Pa*-Ami activity increased as the temperature increased from 30 to 50 °C. The purified *Pa*-Ami exhibited a maximum activity at 50 °C and the enzymatic activity sharply decreased above the optimum temperature (50 °C) (Fig. 4).

*3.5 Optimization of substrate loading*

Whole cell biocatalyst has a series of advantages over isolated enzymes, and has been widely adopted for the commercial production of bulk chemicals and valuable pharmaceuticals [27-29]. Therefore, whole cells of *E. coli* overexpressing *Pa*-Ami were used to catalyze the hydrolysis of 1-CCHAM at 35 °C and pH 8.5.

High concentration of substrate is beneficial to an industrial bioprocess because of lower catalyst consumption and easier product recovery. However, the substrate concentrations of amidase-catalyzed biotransformation are usually low because of

their toxicity [30, 31]. In this study, the effect of substrate loading on the hydrolytic reaction was investigated. As shown in Fig. 5, the whole-cell biocatalysts (2 g/L, wet cell weight) exhibited strong tolerance against high substrate concentration (up to 100 g/L). The product concentration increased dramatically at the initial stage of the reaction and the conversion reached 100% after 10, 15 and 20 min with 60, 80 and 100 g/L of substrate. However, product formation no longer increased when the substrate concentration was raised up to 150 g/L (data not shown). What's more, the conversion was only 90.1% at the substrate concentration of 150 g/L, even the biocatalyst loading was elevated to 5 g/L and reaction time was prolonged (Table S2). This may be ascribed to the enzyme inactivation caused by a high concentration of product and this type of inhibition has been reported in many enzymatic hydrolysis [32, 33].

*3.6 Optimization of biocatalyst loading*

The amount of biocatalyst used was another crucial factor for its potential application. The influence of biocatalyst loading on the conversion of 1-CCHAM (100 g/L) was investigated. As depicted in Fig. 6A, a conversion of 100% was obtained with 2 and 3 g/L wet whole cells. The time required for complete conversion was shortened from 20 to 15 min as the amount of biocatalyst increased from 2 to 3 g/L. When biocatalyst loading of 1 g/L was employed, the conversion reached 80% after 20 min and product formation no longer increased. However, 80 g/L substrate could be completely hydrolyzed with 1 g/L biocatalyst loading (a S/C-ratio of 80) after 20 min (Fig. 6B). On the other hand, space-time yield, which presents quantitative data

on the productivity, is the main intensification criterion of the biotransformation itself. A high space-time yield, which could reduce the capital costs of the process, requires a high specific activity of the biocatalyst. This process exhibited a high space-time yield of 5794.7 $g_{product}$ $L^{-1}$ $d^{-1}$, which markedly exceeded the average one of industrial bioprocess (372 $g_{product}$ $L^{-1}$ $d^{-1}$) [34].

*3.7 Effect of product concentration on hydrolytic reaction*

Enzymes were shown to be inhibited by their catalyzed product [35]. To investigate the effect of product concentration, the conversion was determined at various initial concentrations of 1-CCHAA (10 to 40 g/L). The conversion significantly decreased from 84.4% to 56.4% when initial concentration of 1-CCHAA was increased from 10 to 40 g/L (Fig. 7).

To explore the inhibition mechanism of *Pa*-Ami, the inhibitory type of 1-CCHAA was investigated by Dixon plots (Fig. 8). The plots of *Pa*-Ami with various concentrations of 1-CCHAA resulted in a family of straight lines intersecting one another above the x-axis, with a *Ki* value of 50.62±6.7 mM. Therefore, the inhibition mode of 1-CCHAA toward *Pa*-Ami was competitive inhibition where 1-CCHAA reversibly binds to an allosteric site on *Pa*-Ami.

**4. Conclusion**

In summary, we have exploited a novel amidase for efficient hydrolysis of 1-CCHAM to afford 1-CCHAA. The recombinant *Pa*-Ami exhibited high hydrolytic activity and strong tolerance against high substrate loading. The biocatalytic process with high S/C-ratio (80) provided a more economical route for industrial application,

resulting in an outstanding space-time yield of 5794.7 $g_{product}$ $L^{-1}$ $d^{-1}$. The developed amidase-catalyzed process avoids the use of strong acids and organic solvent and thus reduces remarkably the toxicity to environment as compared to chemical processes. On the other hand, it significantly improved the catalytic efficiency as compared to previously reported biocatalysts. These encouraging results not only demonstrated the feasibility of in silico mining of novel enzymes based on sequence homology, but also indicated that amidase-catalyzed industrial production of 1-CCHAA is viable, technologically efficient and environmentally benign.

**Acknowledgements**

This work was supported by the National Nature Science Foundation of China (No. 21202150), National Science Foundation of Zhejiang (Y4080334, LY13B060004) and National High Technology Research and Development Program of China (No.2012AA022201B).

**References**

[1] Robinson AA, Malow BA. Gabapentin shows promise in treating pediatric insomnia. Sleep 2012;35:A394-A394.

[2] Segal AZ, Rordorf G. Gabapentin as a novel treatment for postherpetic neuralgia. Neurology 1996;46:1175-1176.

[3] Zapp JJ. Postpoliomyelitis pain treated with gabapentin. Am Fam Physician 1996;53:2442-2444.

[4] Mellick GA, Mellick LB. Reflex sympathetic dystrophy treated with gabapentin. Arch Phys Med Rehab 1997;78:98-105.

[5] Chang CY, Challa CK, Shah J, Eloy JD. Gabapentin in acute postoperative pain management. BioMed Res Int 2014;2014: 631756.

[6] Attal N, Cruccu G, Baron R, Haanpaa M, Hansson P, Jensen TS, Nurmikko T. EFNS guidelines on the pharmacological treatment of neuropathic pain: 2010 revision. Eur J Neurol 2010;17:1113-E1188.

[7] Xu XX, Wei ZL, Bai X. Beckmann rearrangement as a key to gabapentin. Chinese J Org Chem 2006;26:354-356.

[8] Griffiths G, Mettler H, Mills LS, Previdoli F. Novel syntheses of gabapentin via addition of hydrocyanic acid to cyclohexylidenemalonate or cyano(cyclohexylidene)acetate. Helv Chim Acta 1991;74:309-314.

[9] Jennings RA, Johnson DR, Seamans RE, Zeller JR. Process for cyclic amino acid anticonvulsant compounds. USA. Patent. US 5319135. 94.06.07.

[10] Jennings RA, Seamans RE, Zeller JR, Johnson DR. Process for cyclic amino acid

anticonvulsant compounds. Eur. Patent EP 0414262 B1. 94.11.30.

[11] Zhu D, Mukherjee C, Biehl ER, Hua L. Nitrilase-catalyzed selective hydrolysis of dinitriles and green access to the cyanocarboxylic acids of pharmaceutical importance. Adv Synth Catal 2007;349:1667-1670.

[12] Wong JW, Burns MP. Biocatalytic preparation of 1-cyano-cyclohexaneacetic acid. USA. Patent. US 20050009154 A1. 05.01.13.

[13]Xue YP, Wang YP, Xu Z, Liu ZQ, Shu XR, Jia DX, Zheng YG, Shen YC. Chemoenzymatic synthesis of gabapentin by combining nitrilase-mediated hydrolysis with hydrogenation over Raney-nickel. Catal Commun 2015;66:121-125.

[14]Xue YP, Zheng YG, Wang YP, Zou SP. Chemo-enzymatic synthesis of gabapentin. CHN. Patent. CN104911225A 2015.09.16.

[15] Zheng RC, Yin XJ, Zheng YG. Highly regioselective and efficient production of 1-cyanocyclohexaneacetamide by *Rhodococcus aetherivorans* ZJB1208 nitrile hydratase. J Chem Technol Biotechnol 2015; DOI: 10.1002/jctb.4724.

[16] Burns MP, Weaver JK, Wong JW, John WW, Justin KW, Michel PB. Stereoselective bioconversion of alphatic dinitriles into cyano carboxylic acids. EUR. Patent. WO2005100580-A1. 2005.10.27

[17] Villalobos A, Ness JE, Gustafsson C, Minshull J, & Govindarajan S. Gene designer: A synthetic biology tool for constructing artificial DNA segments. BMC Bioinformatics 2006; 7:2–3.

[18] Chung CT, Niemela SL, & Miller Roger H. One-step preparation of competent

Escherichia coli: Transformation and storage of bacterial cells in the same solution. Biochem 1989;86:2172-2175.

[19] Bradford MM. A rapid and sensitive method for the quantitation of microgram quantities of protein utilizing the principle of protein-dye binding. Anal Biochem 1976;72:248-254.

[20] Hallaway D, Feiner S, Hollerer T. Bridging the gaps: Hybrid tracking for adaptive mobile augmented reality. Appl Artif Intell 2004;18:477-500.

[21] Novo C, Farnaud S, Tata R, Clemente A, Brown PR. Support for a three-dimensional structure predicting a Cys-Glu-Lys catalytic triad for *Pseudomonas aeruginosa* amidase comes from site-directed mutagenesis and mutations altering substrate specificity. Biochem J 2002;365:731-738.

[22] Neumann S, Kula MR. Gene cloning, overexpression and biochemical characterization of the peptide amidase from *Stenotrophomonas maltophilia*. Appl Microbiol Biotechnol 2002;58:772-780.

[23] Cai G, Zhu S, Wang X, Jiang W. Cloning, sequence analysis and expression of the gene encoding a novel wide-spectrum amidase belonging to the amidase signature superfamily from *Achromobacter xylosoxidans*. FEMS Microbiol Lett 2005;249:15-21.

[24] Zheng RC, Zheng YG, Shen YC. Amidase catalyzed kinetic resolution of racemic mandelamide to (*R*)-mandelate by *Delftia tsuruhatensis* ZJB-05174. J Biotechnol 2008;136:S368-S368.

[25] Oinuma K, Takuwa A, Taniyama K, Doi Y, Takaya N. Hydrazidase, a novel

amidase signature enzyme that hydrolyzes acylhydrazides. J Bacteriol 2015;197:1115-1124.

[26] Labahn J, Neumann S, Buldt G, Kula MR, Granzin J. An alternative mechanism for amidase signature enzymes. J Mol Biol 2002;322:1053-1064.

[27] Shaw NM, Naughton A, Robins K, Tinschert A, Schmid E, Hischier ML, Venetz V, Werlen J, Zimmermann T, Brieden W, de Riedmatten P, Roduit JP, Zimmermann B, Neumuller R. Selection, purification, characterisation, and cloning of a novel heat-stable stereo-specific amidase from *Klebsiella oxytoca*, and its application in the synthesis of enantiomerically pure (*R*)- and (*S*)-3,3,3-trifluoro-2-hydroxy-2-methylpropionic acids and (*S*)-3,3,3-trifluoro-2-hydroxy-2-methylpropionamide. Org Process Res Dev 2002;6:497-504.

[28] Yang ZY, Ni Y, Lu ZY, Liao XR, Zheng YG, Sun ZH. Industrial production of *S*-2,2-dimethylcyclopropanecarboxamide with a novel recombinant *R*-amidase from *Delftia tsuruhatensi*s. Process Biochem 2011;46:182-187.

[29] Schmid A, Dordick JS, Hauer B, Kiener A, Wubbolts M, Witholt B. Industrial biocatalysis today and tomorrow. Nature 2001;409:258-268.

[30] Nojiri M, Taoka N, Yasohara Y. Characterization of an enantioselective amidase from *Cupriavidus* sp. KNK-J915 (FERM BP-10739) useful for enzymatic resolution of racemic 3-piperidinecarboxamide. J Mol Catal B-Enzym 2014;109:136-142.

[31] Fuhshuku K, Watanabe S, Nishii T, Ishii A, Asano Y. Efficient preparation of

both enantiomers of 3,3,3-trifluoro-2-hydroxy-2-methylpropanoic acid catalyzed by *Shinella* sp. R-6 and *Arthrobacter* sp. S-2. J Mol Catal B-Enzym 2014;102:115-119.

[32] Xue YP, Liu ZQ, Xu M, Wang YJ, Zheng YG. Efficient separation of (*R*)-(-)-mandelic acid biosynthesized from (*R,S*)-mandelonitrile by nitrilase using ion-exchange process. J Chem Technol Biotechnol 2011;86:391-397.

[33] Hua DL, Lin S, Li YF, Chen H, Zhang ZB, Du Y, Zhang XH, Xu P. Enhanced 2-phenylethanol production from L-phenylalanine via in situ product adsorption. Biocatal Biotransform 2010;28:259-266.

[34] Bommarius AS, Riebel-Bommarius BR, Biocatalysis: fundamentals and applications, John Wiley & Sons; 2007. p. 1–2.

[35] Sonoki T, Morooka M, Sakamoto K, Otsuka Y, Nakamura M, Jellison J, Goodell B. Enhancement of protocatechuate decarboxylase activity for the effective production of muconate from lignin-related aromatic compounds. J Biotechnol 2014;192:71-77.

**Figure captions**:

Fig. 1 Chemoenzymatic route for synthesis of gabapentin

Fig. 2 Docking of 1-CCHAM to the active pocket of the recombinant *Cc*-Ami (A), *Pa*-Ami (B) and *Dt*-Ami 6 (C).

Fig. 3 Effects of pH on activity of the purified *Pa*-Ami. The activities were determined in standard conditions in different buffers with pH varying from 6.0 to 10.0. The enzyme activity obtained in 50 mM Tris-HCl buffer (pH 8.5) was taken as 100%. The buffers: $NaH_2PO_4$-$Na_2HPO_4$ buffer was used for pH 6.0-7.5(■); Tris-HCl buffer for 7.5-9.0(◇); Gly-NaOH for pH 9.0-10.0 (▲).

Fig. 4 Effects of temperature on activity of the purified *Pa*-Ami. Assays were performed at various temperatures (30-65 °C) in Tris-HCl buffer (pH 8.5). The enzyme activity obtained at 50 °C was taken as 100%.

Fig. 5 Time course of 1-CCHAA production by recombinant whole *E. coli* cells at various substrate concentrations. The reactions were performed in 50-mL flasks with 10 mL of reaction mixtures consisted of various substrate concentrations (60-100 g/L), 100 mM Tris-HCl (pH 8.5) and 2 g/L *E. coli* cells at 35 °C.

Fig. 6 (A) Time course of 1-CCHAA production by whole *E. coli* cells at various biocatalyst loadings. The reactions were performed in reaction mixtures consisted of various biocatalyst loading (1-3 g/L), 100 mM Tris-HCl (pH 8.5) and 100 g/L 1-CCHAM at 35 °C; (B) Time course of 1-CCHAA production by 1 g/L whole *E. coli* cells. The reactions were performed in reaction mixtures consisted of 80 g/L 1-CCHAM and 100 mM Tris-HCl (pH 8.5) at 35 °C.

Fig. 7 Effect of concentrations of pre-added 1-CCHAA on conversion. The reactions

were performed in reaction mixtures consisted of various concentrations of 1-CCHAA (10-40 g/L), 100 mM Tris-HCl (pH 8.5), 80 g/L 1-CCHAM and 1 g/L *E. coli* cells at 35 °C.

Fig. 8 Determination of enzyme inhibition characteristics by Dixon plots for 1-CCHAA. *Pa*-Ami activity was measured at different 1-CCHAA concentrations (7.5-240 mM) in the presence of 20 and 40 mM 1-CCHAM.

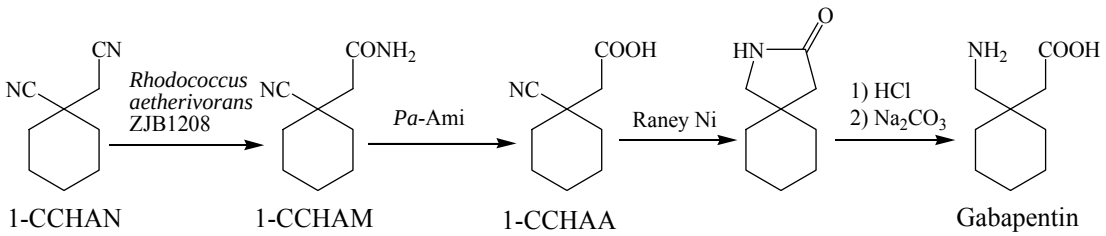


Fig. 1

A

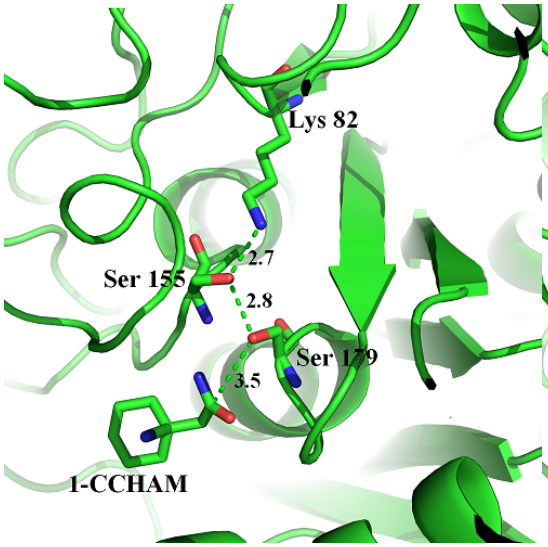


B

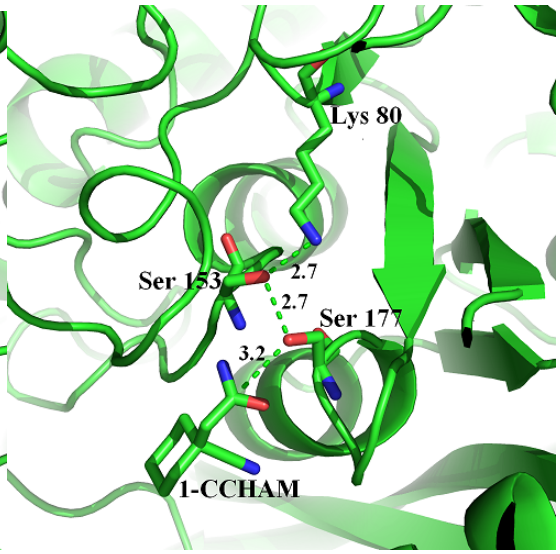


C

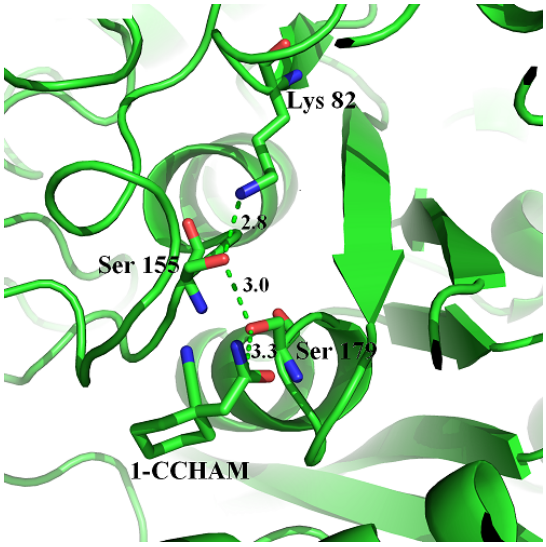


Fig. 2

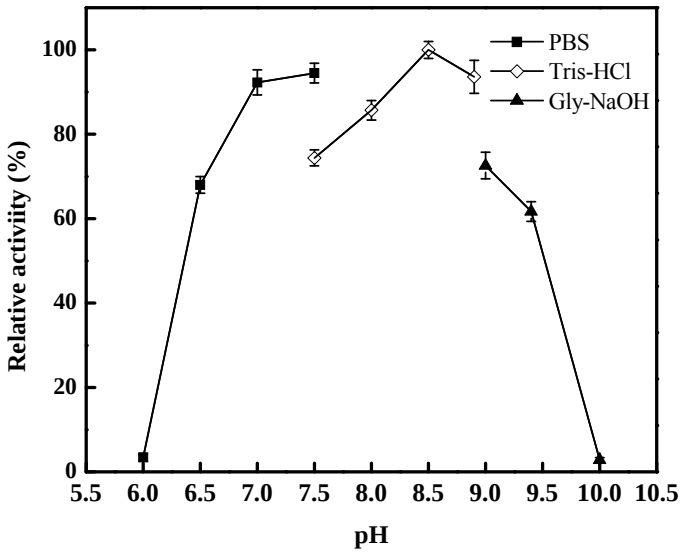


Fig. 3

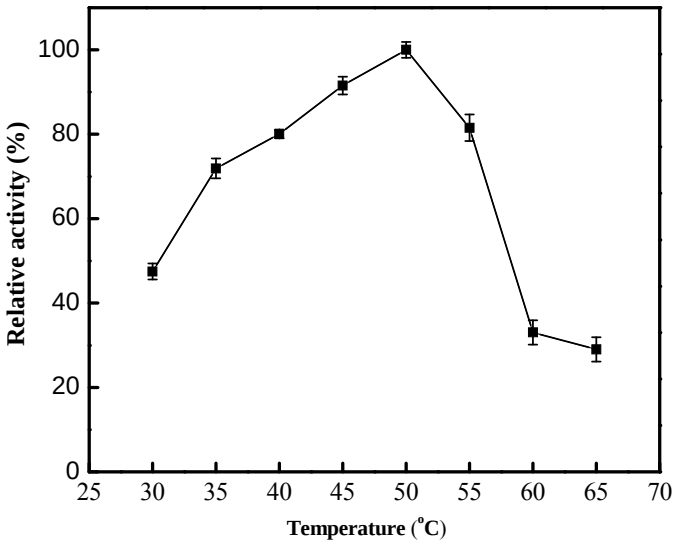


Fig. 4

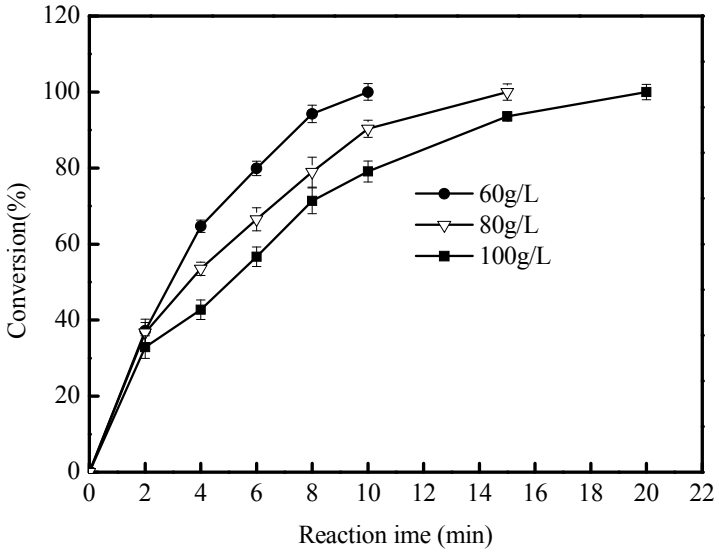


Fig. 5

A

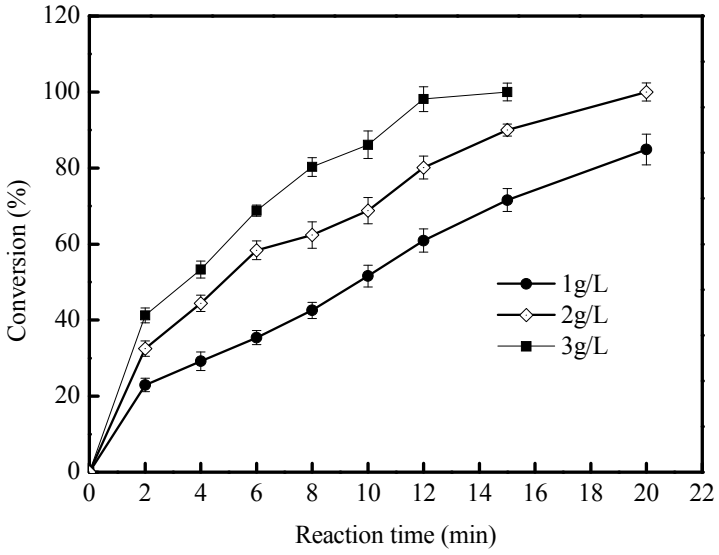


B

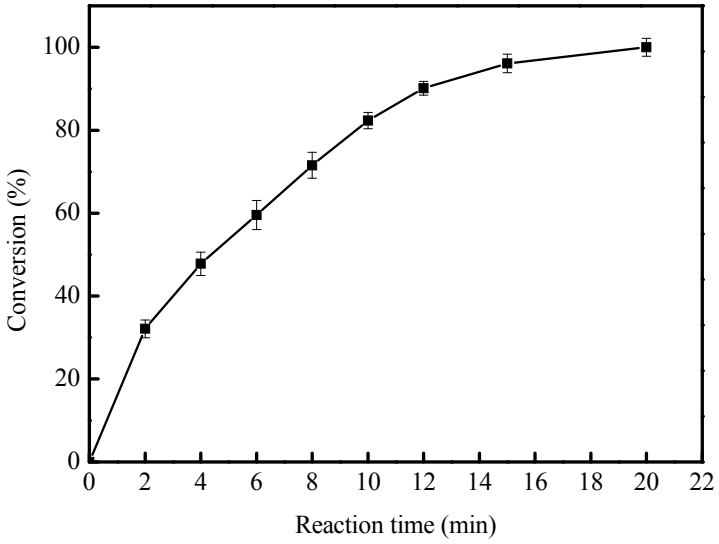


Fig. 6

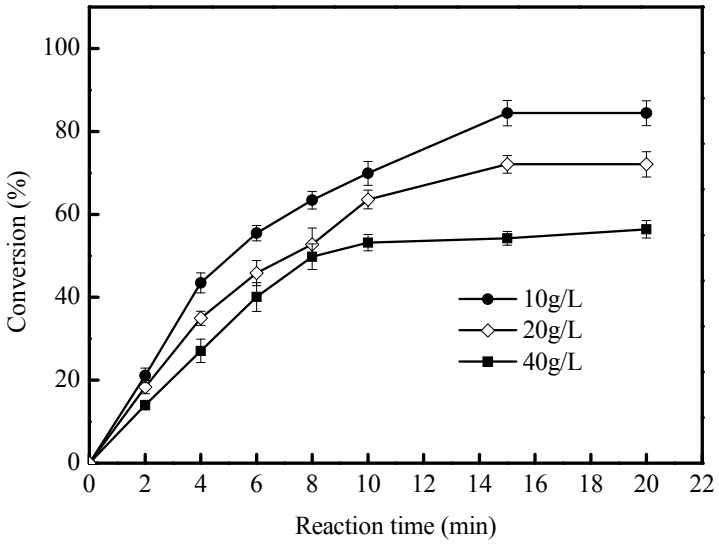


Fig. 7

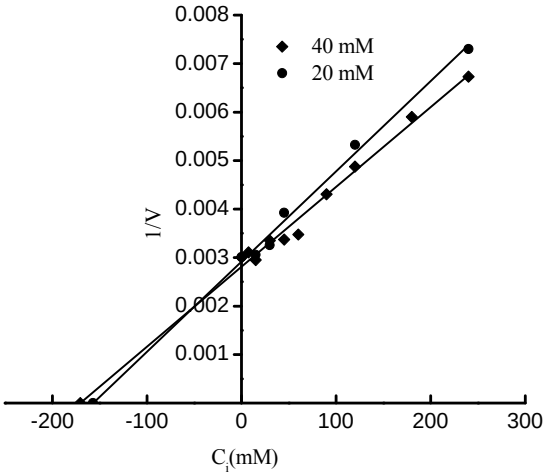


Fig. 8

Table 1. Kinetic parameters of hydrolysis of 1-CCHAM with *Cc*-Ami, *Pa*-Ami and *Dt*-Ami 6.

| Enzyme | $K_m$ (mM) | $V_{max}$ (μmol $mg^{-1}$ $min^{-1}$) | $k_{cat}$ ($s^{-1}$) | $k_{cat}/K_m$ ($s^{-1}mM^{-1}$) |
|---|---|---|---|---|
| *Cc*-Ami | 2.05±0.22 | 46±0.4 | 39±0.3 | 19.3±1.8 |
| *Pa*-Ami | 1.21±0.11 | 300±4.2 | 250.1±3.5 | 208.2±16.2 |
| *Dt*-Ami 6 | 1.77±0.03 | 185.3±4.8 | 160.8±4.1 | 90.9±2.9 |